NAVWEPS REPORT 8169 1 NOVEMBER 1963

NAVWEPS REPORT 8169

SUBMILLIMETER RADIOMETRY

J. W. BATTLES

D. E. CRANE

RESEARCH DEPARTMENT

NAVAL ORDNANCE LABORATORY CORONA

CORONA, CALIFORNIA

NAVAL ORDNANCE LABORATORY CORONA

W. R. KURTZ, CAPT., USN
Commanding Officer

F. S. ATCHISON, Ph. D.
Technical Director

ABSTRACT

This report discusses some of the problems involved in defining the parameters of a submillimeter radiometer. Areas in which there is a need for experimental measurements are outlined, a short survey is given of millimeter and submillimeter wave components, and future plans of the submillimeter research program are discussed.

FOREWORD

As authorized by WepTask R360-FR-104/211-1/R011-01-001, the Microwave Systems Branch of the Naval Ordnance Laboratory Corona is conducting studies of millimeter and submillimeter radiometry techniques. As part of these studies, a review of the state of the field is presented in this report. The areas in which research work is needed in order to evaluate millimeter and submillimeter radiometry are discussed. This work began April 1963, and the task is a continuing one.

C. J. HUMPHREYS
Head, Research Department

CONTENTS

INTRODUCTION

Most of the reports that have been written on radiometers designed for use at submillimeter wavelengths discuss them as a tool for studying objects outside the earth's atmosphere. A submillimeter radiometer can, however, also be used to make thermal maps of the earth's surface, to study the moisture content of the atmosphere, and to study changes in the weather.

In making thermal maps of the earth's surface, the submillimeter radiometer has an advantage over the microwave radiometer because a much smaller antenna dish can be used for the same beam width. The atmospheric attenuation at submillimeter wavelengths may greatly reduce the effective range of the submillimeter radiometer, but it is the change in attenuation with a change in moisture that will make the submillimeter radiometer a good tool for the study of weather.

This report will discuss (1) the factors affecting the submillimeter radiometer within the earth's atmosphere, (2) development of submillimeter wave components, and (3) future plans of this research program.

THERMAL RADIATION

BLACKBODIES

The maximum amount of thermal radiation that any body can emit is called blackbody radiation. This limiting quantity is determined by thermodynamic considerations. The closest approximation to blackbody radiation is found inside a closed container, the walls of which are held at a constant temperature. All other physical bodies, when at the same thermal temperature as the blackbody, emit less thermal radiation.

The thermal radiation of a blackbody in the long wavelength region can be approximated by the Rayleigh-Jeans law

$$P(\lambda,T) = \frac{8\pi k}{\lambda^4} T\Delta\lambda \frac{\text{watts}}{\text{m}^2 \text{ steradian}} \qquad (1)$$

where

k = Boltzmann constant (mks)

λ = wavelength (meters)

$\Delta\lambda$ = change in wavelength

T = thermal temperature at which a blackbody would produce $P(\lambda,T)\Delta\lambda$

$P(\lambda,T)\Delta\lambda$ = energy radiated per unit area in 1 sec in 1 steradian

The equation that fits experimental blackbody radiation values at all wavelengths is called Planck's law, and it is written

$$P(\lambda,T)\Delta\lambda = \frac{2c^2h}{\lambda^5}\,\frac{1}{\exp(ch/\lambda kT) - 1}\,\Delta\lambda\,\frac{\text{watts}}{\text{m}^2\ \text{steradian}} \tag{2}$$

where

h = Planck's constant (mks)

c = speed of light (mks)

Later, a discussion will be presented about the wavelengths and the temperatures at which Eq. 2 is approximated by Eq. 1.

GRAY BODIES

A gray body is a body that emits less thermal radiation for a given temperature than a similar blackbody at the same temperature. The thermal energy radiated by a gray body per unit area in 1 sec in 1 steradian between λ and $(\lambda + \Delta\lambda)$ is given by

$$P_G(\lambda,T)\Delta\lambda = \epsilon_G(\lambda)P(\lambda,T)\Delta\lambda \tag{3}$$

The term $\epsilon_G(\lambda)$ is defined as the spectral emissivity of the gray body G, and it has values between 0 and 1. The emissivity can be a function of the position of the observer with respect to the gray body. An example would be a square, flat sheet with high, thin, parallel fins on two of its edges. If the observer were to stand at one side of the sheet, the sheet would present more area to him when the fins were antiparallel to the projection of the observer's line of sight onto the plane of the sheet than when they were parallel to it. Since there is a difference in the area presented to the observer, there would be a difference in the amount of thermal radiation received by him.

The blackbody used here as a reference is a smooth, regular-shaped body. It is easier to measure the emissivity as a function of angle than it is to calculate the blackbody radiation for a rough irregular body. A more detailed discussion of the emissivity can be found in Ref. 1.

SUBMILLIMETER THERMAL RADIATION AT THE RADIOMETER ANTENNA

The total energy received by the radiometer is defined in terms of the radiometric temperature of the energy received from the target and from any other sources. The target is defined as any source of thermal radiation that the radiometer is to observe. All other sources radiating energy directly into the radiometer will be called the background. All sources radiating energy into the radiometer through reflections from the target and the background will be called sky. It is assumed that the antenna beam of the radiometer is a pencil beam with small side lobes.

The rate at which energy is radiated in the direction of the radiometer antenna, $P(\lambda,T)\Delta\lambda$, is defined by

$$P(\lambda,T)\Delta\lambda = P_t\left(\lambda,T_t\right)\Delta\lambda + P_b\left(\lambda,T_b\right)\Delta\lambda + \left[\rho_t(\lambda) + \rho_b(\lambda)\right]P_s\left(\lambda,T_s\right)\Delta\lambda \qquad (4)$$

where

$P_t(\lambda,T_t)\Delta\lambda$ = rate at which energy is radiated from target

$P_b(\lambda,T_b)\Delta\lambda$ = rate at which energy is radiated from background

$P_s(\lambda,T_s)\Delta\lambda$ = rate at which energy is radiated from sky (a radiometric measurement)

$\rho_t(\lambda)$ = reflection coefficient of target; equals $1 - \epsilon_t(\lambda)$

$\rho_b(\lambda)$ = reflection coefficient of background; equals $1 - \epsilon_b(\lambda)$

T_t = thermodynamic temperature of target

T_b = thermodynamic temperature of background

T_s = radiometric temperature of sky

T = radiometric temperature for $P(\lambda,T)\Delta\lambda$

Neither the target nor the background is a blackbody; therefore the rate at which energy is radiated from each is defined in terms of Eq. 3. Equations for $P_t(\lambda,T_t)\Delta\lambda$ and $P_b(\lambda,T_b)\Delta\lambda$ can be written as

$$P_t(\lambda, T_t)\Delta\lambda = \epsilon_t(\lambda)P(\lambda, T_t)\Delta\lambda \tag{5}$$

and

$$P_b(\lambda, T_b)\Delta\lambda = \epsilon_b(\lambda)P(\lambda, T_b)\Delta\lambda \tag{6}$$

Assuming that G = t, b, then $P(\lambda, T_G)$ is the blackbody radiation given by Eq. 2 for a temperature T_G.

Equation 4 can now be written in terms of Eq. 5 and 6, giving

$$P(\lambda, T)\Delta\lambda = \epsilon_t(\lambda)P(\lambda, T_t)\Delta\lambda + \epsilon_b(\lambda)P(\lambda, T_b)\Delta\lambda + \left[\rho_t(\lambda) + \rho_b(\lambda)\right]P_s(\lambda, T_s)\Delta\lambda \tag{7}$$

If we examine Eq. 7 in a given wavelength region, say λ to $(\lambda + \Delta\lambda)$, we find that $P(\lambda, T)\Delta\lambda$ is a function of the temperatures T_t, T_b, and T_s only. Now $\epsilon_t(\lambda)$, $\epsilon_b(\lambda)$, $\rho_t(\lambda)$, and $\rho_b(\lambda)$ have been determined experimentally and can be considered to be known constants. $P_s(\lambda, T_s)$ is also determined experimentally and is defined in terms of a temperature T_s, which is the temperature at which a blackbody would radiate $P_s(\lambda, T_s)$ in the region λ to $(\lambda + \Delta\lambda)$. Equation 7 can be considered to be a function defining the relationships between the temperatures T, T_t, T_b, and T_s. The Rayleigh-Jeans law, Eq. 1, can be used with Eq. 7 to produce an equation that has a linear relationship between the temperatures.

$$T = \epsilon_t T_t + \epsilon_b T_b + \left(\rho_t + \rho_b\right)T_s \tag{8}$$

If Planck's law, Eq. 2, is used, the relationship between the temperatures is linear only in the region where the Rayleigh-Jeans law gives the same value for the radiation as does Planck's law.

It is the value T_t that we are trying to determine. The radiometer measures $P(\lambda, T)\Delta\lambda$, and the other terms are known. If we want T_t to have physical meaning, we must know when to use Eq. 1 and 8. If no physical meaning is necessary, then Eq. 1 and 8 can be used.

The percent error made by using Eq. 1 in place of Eq. 2 for calculating the radiation is given by

$$E = \left|1 - \frac{\lambda kT}{ch}\left[\exp(ch/\lambda kt) - 1\right]\right| 100\% \tag{9}$$

Equation 9 can be used to determine the region where Eq. 8 has physical meaning. In Fig. 1, which is a graph of Eq. 9, the product λT is used as the variable. In Fig. 2, which is a plot of Eq. 9 for several values of T, λ is used as the variable. These graphs show the submillimeter region as the region where Eq. 1 begins to produce a large error for temperatures less than 500°K. When the exponential in Eq. 9 is expanded in a Taylor series, we find that if the error E is to be small we must have

$$\frac{ch}{k} \ll \lambda T \tag{10}$$

The use of Eq. 1 to calculate T from the measured quantity $P(\lambda,T)\Delta\lambda$ will give a value for T less than or equal to the true value; that is, less than or equal to the value that Eq. 2 would give. Thus, when we use Eq. 8 to find T_t, we always find a value for T_t that is less than or equal to the true thermal temperature of the target.

The next step is to consider the path that the radiation takes from the target to the radiometer. The radiation given by Eq. 7 is reduced by atmospheric attenuation and by the solid angle that the emitting surface subtends at the antenna. Thus, the power received by the antenna is

$$\mathbb{P} = \gamma \int_{\Omega} A_e(\theta,\phi) P(\lambda,T)\, d\Omega\Delta\lambda + \mathbb{P}_s \tag{11}$$

where

$\mathbb{P}$ = total power received by antenna

$\mathbb{P}_s$ = power radiated directly into antenna by atmosphere

$A_e(\theta,\phi)$ = effective antenna area

$P(\lambda,T)\Delta\lambda$ = radiation energy defined by Eq. 7

Ω = solid angle of antenna beam

γ = atmospheric attenuation

$d\Omega$ = differential solid angle

When Eq. 7 and Planck's law, Eq. 2, are used to evaluate Eq. 11, we see that there are four integrals to evaluate, two over the target area and two over the background area. It is best to consider the integrals one at a time. First, the power radiated by the target is

$$\mathbb{P}_1 = \gamma \int_{\Omega_t} A_e(\theta,\phi)\epsilon_t(\lambda) P\left(\lambda,T_t\right) d\Omega\Delta\lambda$$

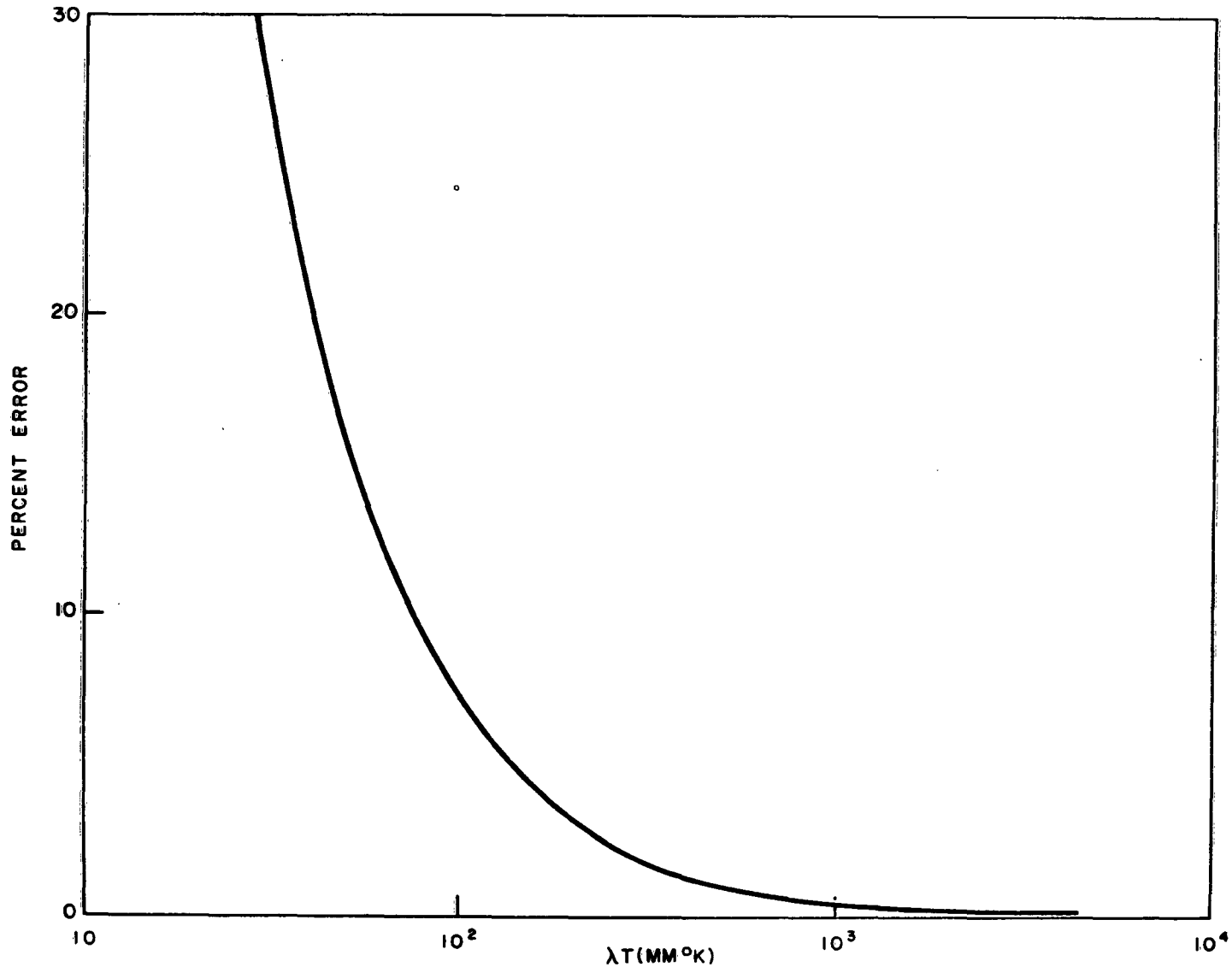

FIGURE 1. Percent Error as a Function of the Product λT in Calculating the Power Radiated in $\lambda \rightarrow (\lambda + \Delta\lambda)$ by Using the Rayleigh-Jeans Law in Place of Planck's Law

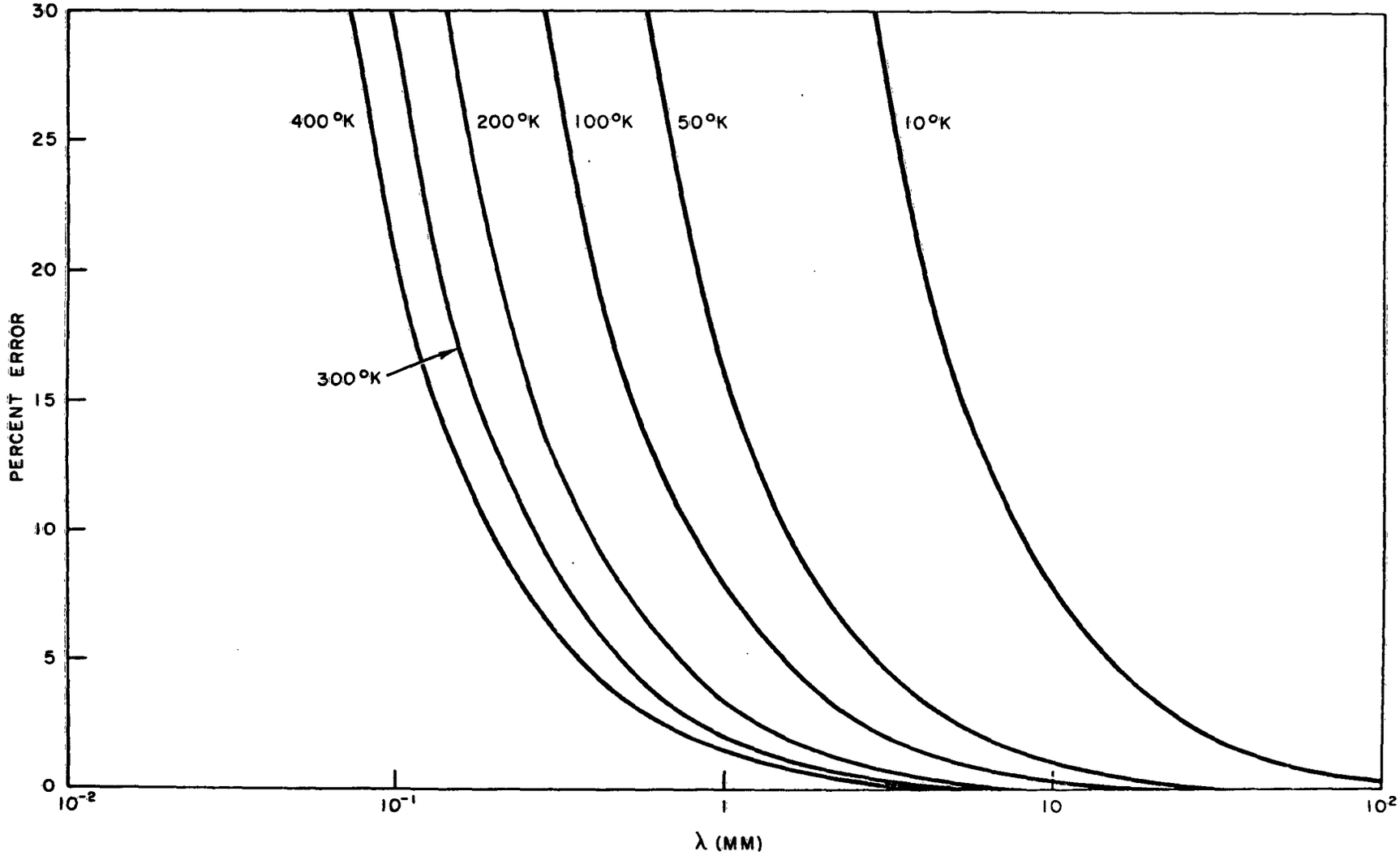

FIGURE 2. Percent Error as a Function of λ for Fixed Temperatures in Calculating the Power Radiated in $\lambda \rightarrow (\lambda + \Delta\lambda)$ by Using the Rayleigh-Jeans Law in Place of Planck's Law

where Ω_t is the solid angle of the target. Using Planck's law, we get

$$\mathbb{P}_1 = \gamma 2c^2 h \int_{\Omega_t} A_e(\theta,\phi)\left[\frac{\epsilon_t(\lambda)}{\lambda^5}\right]\left[\frac{1}{\exp\left(ch/\lambda k T_t\right) - 1}\right] d\Omega\Delta\lambda$$

If we assume that $\epsilon_t(\lambda)$ and T_t are constant over the surface of the target, then

$$\mathbb{P}_1 = \gamma\left(\frac{2c^2 h}{\lambda^5}\right)\left[\frac{\epsilon_t(\lambda)\Delta\lambda}{\exp\left(ch/\lambda k T_t\right) - 1}\right]\int_{\Omega_t} A_e(\theta,\phi)\, d\Omega \tag{12}$$

Now $A_e(\theta,\phi)$ is defined in terms of the antenna gain (Ref. 2) by

$$A_e(\theta,\phi) = \frac{\lambda^2}{4\pi} G(\theta,\phi)$$

Thus

$$\int_{\Omega_t} A_e(\theta,\phi)\, d\Omega = \frac{\lambda^2}{4\pi}\int_{\Omega_t} G(\theta,\phi)\, d\Omega$$

and Eq. 12 becomes

$$\mathbb{P}_1 = \gamma\left(\frac{c^2 h}{2\pi\lambda^3}\right)\left[\frac{\epsilon_t(\lambda)\Delta\lambda}{\exp\left(ch/\lambda k T_t\right) - 1}\right]\int_{\Omega_t} G(\theta,\phi)\, d\Omega \tag{13}$$

Because the temperature T_b is not necessarily constant over the background, the power radiated by the background $\mathbb{P}_2$ is given by

$$\mathbb{P}_2 = \gamma\left(\frac{c^2 h}{2\pi\lambda^3}\right)\int_{\Omega_b}\left[\frac{\epsilon_b(\lambda)\Delta\lambda}{\exp\left(ch/\lambda k T_t\right) - 1}\right] G(\theta,\phi)\, d\Omega \tag{14}$$

where Ω_b is the solid angle of the background. The last two integrals represent the power reflected into the antenna from the target and the background. Since $\rho_t(\lambda)$ and $\rho_b(\lambda)$ are assumed constant in the antenna beam, we get

$$\mathbb{P}_3 = \gamma\rho_t(\lambda)\int_{\Omega_t} A_e(\theta,\phi)P_s(\lambda,T_s)\Delta\lambda\, d\Omega$$

and

$$\mathbb{P}_4 = \gamma\rho_b(\lambda)\int_{\Omega_b} A_e(\theta,\phi)P_s(\lambda,T_s)\Delta\lambda\, d\Omega$$

where $P_s(\lambda,T_s)$ is a function of the portion of the sky that is reflected into the radiometer. Since we have assumed the beam width of the antenna to be small, we can assume that $P_s(\lambda,T_s)$ does not change over the antenna beam. Now, $\mathbb{P}_3$ and $\mathbb{P}_4$ can be written

$$\mathbb{P}_3 = \gamma\rho_t(\lambda)P_s(\lambda,T_s)\frac{\lambda^2}{4\pi}\int_{\Omega_t} G(\theta,\phi)\, d\Omega$$

$$\mathbb{P}_4 = \gamma\rho_b(\lambda)P_s(\lambda,T_s)\frac{\lambda^2}{4\pi}\int_{\Omega_b} G(\theta,\phi)\, d\Omega$$

$\mathbb{P}_s$ depends on the distance between the target and the radiometer and must be determined experimentally.

The change in the power received at the antenna because of the appearance of the target in the antenna beam is the difference between the power received when the target and the background are in the beam and the power received when just the background is in the beam. The power change $\Delta\mathbb{P}$ is given by

$$\Delta\mathbb{P} = \mathbb{P}_1 + \mathbb{P}_2 + \mathbb{P}_3 + \mathbb{P}_4 - \mathbb{P}_2' - \mathbb{P}_4'$$

where

$$\mathbb{P}_2' = \gamma\left(\frac{c^2h}{2\pi\lambda^3}\right)\int_{\Omega}\left[\frac{\epsilon_b(\lambda)\Delta\lambda}{\exp\left(ch/\lambda kT_b\right) - 1}\right]G(\theta,\phi)\, d\Omega$$

and

$$\mathbb{P}'_4 = \gamma\rho_b(\lambda)P_s\left(\lambda, T_s\right)\frac{\lambda^2}{4\pi}\int_\Omega G(\theta,\phi)\, d\Omega$$

Combining $\mathbb{P}_2$ with $\mathbb{P}'_2$, and $\mathbb{P}_4$ with $\mathbb{P}'_4$, using Eq. 2 (letting T_b be constant over the background), and using the equality $\rho(\lambda) = 1 - \epsilon(\lambda)$, $\Delta\mathbb{P}$ becomes

$$\Delta\mathbb{P} = \frac{\gamma\lambda^2}{4\pi}\left\{\epsilon_t(\lambda)P\left(\lambda, T_t\right) - \epsilon_b(\lambda)P\left(\lambda, T_b\right)\right. \tag{15}$$

$$\left. + \left[\epsilon_b(\lambda) - \epsilon_t(\lambda)\right]P_s\left(\lambda, T_s\right)\right\}\int_{\Omega_t} G(\theta,\phi)\, d\Omega$$

The effective area A of the antenna beam that is intersected by the target is

$$\frac{\lambda^2}{4\pi}\int_{\Omega_t} G(\theta,\phi)\, d\Omega$$

If we assume the gain of the antenna to be constant across its beam width, then A is just the ratio of the solid angle of the target to the solid angle of the beam, and this ratio (Ref. 3) is given by

$$A = \frac{4A_t}{\pi B^2 r^2}\cos\theta \tag{16}$$

where

A_t = area of target

θ = look angle of radiometer

B = beam width of antenna

r = distance between target and radiometer

Using Eq. 15 and 16, $\Delta\mathbb{P}$ becomes

$$\Delta\mathbb{P} = \gamma\left(\frac{4A_t}{\pi B^2 r^2}\right)\cos\theta\left\{\epsilon_t(\lambda)P\left(\lambda,T_t\right) - \epsilon_b(\lambda)P\left(\lambda,T_b\right) + \left[\epsilon_b(\lambda) - \epsilon_t(\lambda)\right]P_s\left(\lambda,T_s\right)\right\} \tag{17}$$

When the Rayleigh-Jeans law can be used, Eq. 17 reduces to a simple function of temperatures.

$$\Delta T = \gamma\left(\frac{4A_t}{\pi B^2 r^2}\right)\cos\theta\left\{\epsilon_t(\lambda)T_t - \epsilon_b(\lambda)T_b + \left[\epsilon_b(\lambda) - \epsilon_t(\lambda)\right]T_s\right\} \tag{18}$$

It is this equation that is used in the discussions on microwave radiometer mapping and, under certain temperature conditions (see section on blackbody radiation), for submillimeter waves.

EFFECTS OF THE ATMOSPHERE

Equation 17 shows that the radiation power falls off as $1/r^2$. A more important reduction in the radiation is from the atmospheric attenuation γ. The rotational and vibrational frequencies of the oxygen and water vapor molecules of the atmosphere are in the 1-millimeter and the submillimeter regions, and they have a strong absorption effect on any radiation at these frequencies. Fog and rain are s.rong attenuators of submillimeter radiation.

The atmosphere is also a source of radiation. Equation 11 accounts for this source by the term $\mathbb{P}_s$, which depends on the distance between the radiometer and the target, the reflectivity of the target and the background, the amount of moisture in the atmosphere, and the frequency at which the radiometer is operating.

The atmospheric absorption of submillimeter radiation has been calculated theoretically and plotted (Ref. 4 and 5). Theoretical predictions of the oxygen absorption lines agree quite well with experimental results, but the presence of water vapor introduces theoretically unpredicted nonlinearities into the absorption curves. It is believed that either there are unpredicted water vapor lines or there are changes in widths of the oxygen lines caused by the presence of the water vapor. The theoretical results indicate that there should be windows near 94, 140, 240, 400, 660, and 860 Gc. There is some experimental evidence (Ref. 6, 7, 8)

that a window does exist at 860 Gc. The absorption per kilometer in the windows depends on the moisture content of the atmosphere. Iaroshovskii and Stanevich (Ref. 7) gave quantitative data on the absorption, but the path length (7.5 m) was so small that the information is not reliable. To clear up the problems of gaseous absorption in the atmosphere, a controlled experimental program is necessary. Such a program would require a long test cell in which each gas of the atmosphere could be measured for attenuation under various pressures either separately or in different combinations. The measurements that have been made in the atmosphere are good only for predicting attenuation under conditions similar to those of the experiment. The main problem in applying the results from such measurements is that the water-vapor density is usually known only at the transmitter and receiver. Any variation in the water-vapor density along the transmission path would give misleading data. Because of the lack of strong sources in the submillimeter region, it will be necessary to use great care in selecting the cell design. The cell will have to be a low-loss transmission line that can be evacuated.

The appearance of rain or fog in the antenna beam would greatly affect the operation of the radiometer. Figure 3 shows the theoretical attenuation caused by rain and fog for wavelengths greater than 1 mm. There are no experimental measurements of attenuation due to fog or rain for wavelengths shorter than 3 mm. Anderson et al. (Ref. 9) made rain attenuation measurements at 24 Gc in Hilo, Hawaii. They reported that although the annual rainfall there is more than 250 in., the uniformity of the rainfall rarely lasts longer than 1 min. In measuring rain attenuation of submillimeter waves, such nonuniformity of rainfall would be a serious problem, because of the long integration times required. Therefore, to acquire accurate data for rain attenuation of submillimeter waves, it may be necessary to produce rain artificially in the laboratory. The rate of rainfall and the drop size could then be controlled over long periods of time.

The intensity of the submillimeter radiation emitted by the atmosphere depends on the water-vapor density. A plot of the atmospheric radiation intensity against frequency should give maximums at the same frequencies as the maximums of the atmospheric absorption. To develop submillimeter technology, a sound experimental program for studying the variation in atmospheric radiation with water-vapor density and frequency is needed. A basic step in carrying out such a program would be the construction and calibration of a submillimeter radiometer that could be used to make radiometric maps and to study weather changes. Since most weather changes are accompanied by a change in water-vapor density, and since the submillimeter radiometer could be used to observe these density changes, it could become a valuable tool in the study of atmosphere dynamics.

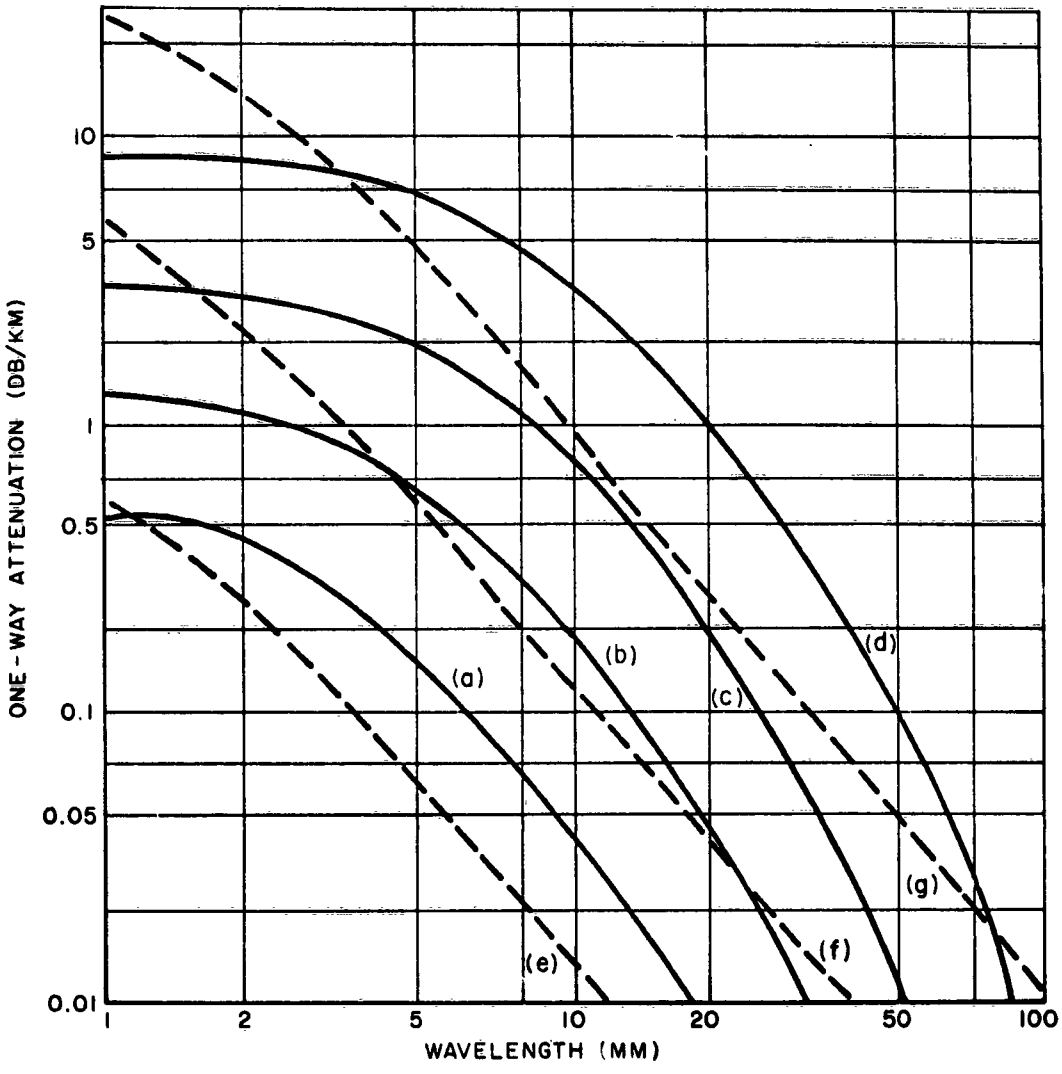

(a) 0.25 MM/HR (DRIZZLE)
(b) 1 MM/HR (LIGHT RAIN)
(c) 4 MM/HR (MODERATE RAIN)
(d) 16 MM/HR (HEAVY RAIN)
(e) 0.032 G/M^3 (VISIBILITY ABOUT 2000 FT)
(f) 0.32 G/M^3 (VISIBILITY ABOUT 400 FT)
(g) 2.3 G/M^3 (VISIBILITY ABOUT 100 FT)

FIGURE 3. Theoretical Values for Attenuation by Rain and Fog. (Solid curves show attenuation in rain of intensity; dashed curves show attenuation in fog or cloud.)

THE SUBMILLIMETER RADIOMETER

The most feasible submillimeter radiometer at this time is the direct-detection radiometer. However, advances in submillimeter amplifiers may, in the near future, make the Dicke type of superheterodyne radiometer more sensitive.

The sensitivity of a radiometer can be found by using Eq. 11, with the restriction that the target fills the antenna beam. Equation 11 now becomes

$$\mathbb{P} = \gamma\epsilon_t(\lambda)\frac{2c^2h}{\lambda^3}\frac{\Delta\lambda}{\exp\left(ch/\lambda kT_t\right) - 1}$$

The change in power with a change in temperature for a radiometer that detects only one polarization is

$$\Delta\mathbb{P} = \frac{\partial\mathbb{P}}{\partial T}\Delta T_t$$

Thus the minimum detectable change in power is

$$\Delta\mathbb{P}_{min} = \gamma\epsilon_t(\lambda)\frac{c^2h\Delta\lambda}{\lambda^3}\frac{\left(ch/\lambda kT_t^2\right)\exp\left(ch/\lambda kT_t\right)}{\left[\exp\left(ch/\lambda kT_t\right) - 1\right]^2}\Delta T_{t(min)}$$

This equation assumes that the target is a gray body and the radiometer is looking through the atmosphere. The minimum detectable change in power $\Delta\mathbb{P}_{min}$ is determined by the components of the radiometer and is known; the minimum detectable target temperature change $\Delta T_{t(min)}$ is the value that is calculated. It is given by

$$\Delta T_{t(min)} = \frac{\lambda^4 kT_t^2\left[\exp\left(ch/\lambda kT_t\right) - 1\right]^2\exp\left[-\left(ch/\lambda kT_t\right)\right]}{\gamma\epsilon_t(\lambda)c^3h^2\Delta\lambda}\Delta\mathbb{P}_{min} \qquad (19)$$

Equation 19 gives the minimum detectable change in target temperature for an arbitrary target radiating through the atmosphere. The minimum detectable temperature of a radiometer ΔT_{min} is usually defined in terms of a blackbody target with no atmospheric attenuation and is given by

$$\Delta T_{min} = \frac{\lambda^4 h T^2}{c^3 h \Delta\lambda} [\exp(ch/\lambda kT) - 1]^2 \exp\left[-\left(ch/\lambda kT_t\right)\right] \Delta \mathbb{P}_{min} \qquad (20)$$

If the Rayleigh-Jeans law can be used, Eq. 20 becomes

$$\Delta T_{min} = \frac{\Delta \mathbb{P}_{min}}{k\Delta f} \qquad (21)$$

Table 1 gives the minimum detectable temperature for a radiometer using various types of detecting elements and operating at 300 Gc with a bandwidth Δf of 100 Gc. Equation 21 was used as the basis for this table, and it is assumed that there were no losses from the antenna to the detector other than polarization. A comparison of Eq. 20 with Eq. 21 shows that if the Rayleigh-Jeans law cannot be used, then ΔT_{min} increases with temperature and wavelength. Since all physical bodies are not blackbodies, Eq. 19 must be used to determine the minimum detectable temperature for a specific target in the atmosphere. If the Rayleigh-Jeans law holds for the target, then Eq. 19 can be reduced in form to

$$\Delta T_{t(min)} = \frac{1}{\gamma \epsilon_t(\lambda)} \frac{\Delta \mathbb{P}}{k\Delta f} \qquad (22)$$

A comparison of Eq. 19 and 22 with Eq. 20 and 21, respectively (using the fact that γ and $\epsilon_t(\lambda)$ are positive numbers less than or equal to 1), shows that a gray body will have a higher minimum detectable temperature than a blackbody. This increase in $\Delta T_{t(min)}$ could become quite large for low temperatures, short wavelengths, and low emissivity.

TABLE 1. Comparison of the Efficiency of Several Detecting Elements

Radiometer operating at 300 Gc with a bandwidth of 100 Gc.

Detector	$\Delta \mathbb{P}_{min}$ (watt)	ΔT_{min} (°K)
Golay cell	2×10^{-10}	146
Thermopile	7×10^{-11}	51
Bolometer	4×10^{-11}	29
Putley	2×10^{-12}	1.5

The function that a given submillimeter radiometer is to perform will determine its basic design. A mapping radiometer would require a wide bandwidth and would have to operate at one of the attenuation windows. These requirements are not always compatible, because if the window is narrow then the bandwidth of the radiometer must also be narrow. A weather radiometer should be tunable over a wide frequency range and should have a narrow bandwidth. This could be done by using an interferometer submillimeter radiometer, or several narrow-band radiometers each with a long integrating time.

SUBMILLIMETER COMPONENTS

Rapid changes in the state of the art of radiometers usable at millimeter and submillimeter wavelengths call for a careful evaluation of available components and apparent limitations in each. Although this is important for all forms of research hardware, it is especially necessary when investigating a new system, rather than attempting to improve an existing system. Some of the components discussed are not commercially available, but are laboratory models, items under development, or devices used for other instrumentation.

In most radiometer, radar, and microwave communication systems now existing, the electromagnetic energy is propagated through conventional waveguides over short distances. At these relatively long wavelengths attenuation and manufacturing methods are not a serious problem. Standard rectangular waveguide and microwave components capable of propagating the dominant TE_{10} mode are readily available. At the shorter millimeter and submillimeter wavelengths, however, the attenuation becomes so great and operating dimensions and tolerances become so small that research personnel are forced to investigate more efficient methods of propagation.

It has been known for some time that for a given circular waveguide size the attenuation for the TE_{01} mode decreases as the wavelength decreases. However, the circular waveguide will sustain many different modes, and investigation has shown it difficult to maintain the low-loss TE_{01} mode of operation.

Another way to reduce the attenuation of enclosed waveguides is to use an oversize waveguide. As in the circular guide, the increased waveguide size allows multimode operation with its inherent problems of mode conversion.

Sommerfeld (Ref. 10) investigated the use of an uncoated cylindrical wire of finite conductivity for use as a transmission line and found that it exhibited low-loss characteristics. The line had a large radial field and consequently any object close to the line would cause field distortions. Non-supported lines would sag, and energy would be lost because it would not follow the curvature of the line. If the line were supported, then reflections and losses would exist. The loosely bound field would preclude use of the line where any bends or changes in direction were necessary.

Goubau (Ref. 11) modified the line by applying a dielectric coating to the line to confine the field. The field was confined as expected, but the coating resulted in much greater attenuation for the line. This line was also susceptible to the losses noted for an uncoated line, both with and without supports.

Pure dielectric waveguides have been tested and found to have low-loss characteristics. However, they exhibit considerable losses from the effects of sagging and reflections from supports, as in the conductive material lines. Also under investigation are dielectric image lines in which a thin strip of low-loss dielectric material is bonded to a flat metal image plane. Low attenuation is achieved below 150 Gc, but as the frequency is increased the dielectric cross section becomes so small that construction and bonding to the image plane become impractical.

All the surface wave transmission lines mentioned above exhibit low-loss attenuation characteristics until the frequency reaches a point where surface roughness becomes a problem.

Two other surface transmission arrangements should be mentioned. The H guide—a surface line that eliminates the problem of support found in the conducting and dielectric lines at the lower frequency end of the spectrum—consists of a rectangular dielectric slab between two parallel conducting planes. It has good possibilities for system applications, but as the frequency is increased, the dielectric slab must become very thin, and then the conducting plane will no longer be self-supporting. The trough guide—an H guide modification that consists of a third wall—not only provides support for the dielectric material, but also suppresses many of the higher order modes that will propagate in the H guide. In appearance, the trough guide resembles half an H guide.

In working with the surface wave transmission lines, great care must be exercised in launching the energy down the line and collecting it efficiently. If transmission over long distances is attempted, inefficient launching could possibly be tolerated. However, over short distances, the sum of the losses from launching, collecting, and transmission might

be greater than the transmission losses from a standard enclosed waveguide, and result in no advantage whatsoever.

Several methods of optical transmission have been investigated. One of these methods employs a system of lenses in which each successive lens forms an image of the source. The quality of the image deteriorates rapidly, however, because the reimaging necessary in a line of even moderate length deforms the image so that the energy cannot be efficiently recovered.

An optical transmission line that has been quite successful and has very good possibilities in the submillimeter region has recently been developed by Goubau et al. (Ref. 12, 13). It is described as a beam waveguide in which a transmitted beam of energy is kept well collimated by a system of lenses. The lenses used by Goubau are designed to shift the phase of the spreading energy so that the phase distribution of a new Fresnel zone is created, as in the original. These phase-correcting lenses are commonly referred to as phase transformers. The first position and maximum spacings of the phase transformers are determined by the aperture of the energy source and the frequency of operation, but these positions have not been found to be extremely critical. Some measurements have disclosed attenuations as low as 32 db per 100 ft at 150 Gc as compared with a theoretical value of 270 db per 100 ft for dominant mode transmission in RG-135U rectangular waveguide at this frequency. The beam waveguide could also be used inside large diameter pipe, which would act as a shield.

Losses in the beam waveguide result primarily from diffraction losses and lens absorption. Absorption losses can be minimized by constructing the phase transformers from material with a high dielectric constant to reduce the thickness. The diffraction losses will then be increased, but these can be reduced by suitable surface treatment. The surface treatment will cause the beam to be frequency-dependent; however, within the limitations of the phase transformer design, the beam waveguide is not frequency-dependent without surface treatment.

Launching electromagnetic energy down the beam waveguide transmission line is typically performed with standard microwave horn and lens systems. Collecting and launching efficiencies appear to be much better than transitions to surface guides. Many components incorporating quasi-optical techniques have been constructed for direct use with the beam waveguide. Among these are attenuators, duplexers, directional couplers, and filters. Most components normally required for microwave systems can be duplicated by using quasi-optical techniques.

As research is pushed further into the region of shorter wavelengths and the use of optical paths for transmission lines is incorporated, it is

inevitable that new lens techniques will be developed for shaping and collimating the electromagnetic beam. Although fuzed quartz has been used for lens construction in the millimeter and shorter wavelengths, there is also extensive use of dielectric materials that are in some cases opaque at optical wavelengths. At these short wavelengths, most of these materials combine relatively low losses with good structural properties and are easy to work with. Teflon, Rexolite, and polystyrene have been used extensively as lens materials.

An interesting lens development that has received widespread use in the millimeter region is the zone plate constructed by Lord Rayleigh for his optical experiments. For a given dielectric material, the thickness, and therefore the absorption losses, can be substantially reduced by constructing a zone plate, rather than a conventional lens configuration. Zone plate theory and construction have been covered quite extensively in various reports and therefore will not be discussed here.

Various writers have noted that certain dielectric materials have opaque or transparent qualities at certain discrete frequencies. However, to the authors' knowledge, very little has been published about the qualitative values of loss tangents and dielectric constants for various materials in the millimeter region. This information is very important when one is faced with the problem of choosing window or lens materials for use in low-loss systems.

For certain system measurements, it may be desirable to investigate only a narrow band of frequencies. This becomes very important in the case of a wide-band source of energy in which a coherent source is desired. Filtering may allow these wide-band sources to be used for measurements if appropriate filtering can be accomplished. However, quite different filtering techniques are required in the submillimeter region. Filters that have been used successfully are echelon gratings, Fabry-Perot plates, zone plates and variations of each of these. Very high Q's have been obtained with the Fabry-Perot plates, which are used quite extensively to reduce second- and third-order effects from submillimeter systems. Other techniques have been used with varying amounts of success. Some have shown promise of further development, but others have been found to be either very broad-band or susceptible to noise contributions from vibration.

While research is being carried on to develop components and systems that will operate in higher frequencies, manufacturing concerns are being hard pressed to supply microwave energy sources at the higher power levels and higher frequencies. Although recently developed reflex klystrons give milliwatt outputs to 140 Gc, they are expensive, and delivery schedules on such units cannot be expected to be as good as on klystrons that operate at a lower frequency, and are more easily produced.

Magnetrons with an upper range of 100 Gc in the killowatt power capacity are said to be available. This energy source is not used in the laboratory so extensively as the klystron, but it may find much use in the communications and radar fields. Carcinotrons are being developed that will have a maximum frequency exceeding 300 Gc at the fundamental and 600 Gc at the first harmonic. Again, the cost of such an item makes it very difficult for some laboratories to procure. If a coherent source for submillimeter use is required, the alternatives are to obtain what is available or to use a means of frequency multiplying and a klystron operating at some lower frequency.

Because of the cost and/or delays in obtaining fundamental submillimeter energy sources, most research near and above 100 Gc is carried out with harmonic generators, and the fundamental frequency is supplied by reflex klystrons operating between 10 and 100 Gc. The energy is supplied to a nonlinear element that has outputs at harmonics of the klystron. Because of the low power from the driving klystron and the losses in harmonic generation, frequency limitations are soon reached where usable output power is available.

With crystal harmonic mixing, the effects of conversion losses cannot be offset by increasing the fundamental signal level, since the crystal will not handle large amounts of power without being damaged. In addition, as the klystron power level is increased, the coherent power-to-noise ratio becomes much less. The crystal harmonic generator is therefore used only as a low-level device, since its output power is less than that required for its use as a local oscillator.

The harmonic generator and crystal mixer have not developed to the point where the combination can be constructed and made to operate without some cut-and-try techniques. In most cases, a considerable number of crystal diodes have to be fabricated to get satisfactory operation at a given frequency. In normal use the life of a good crystal diode is usually a matter of weeks. When the output from the harmonic generator starts to deteriorate or the harmonic being used is changed, the diode junction has to be changed for optimum output.

Research with ferrite harmonic generation is also being conducted. The ferrite generators are being driven with magnetrons in order to take advantage of the higher power input capability. The state of the art in this area is such that the efficiencies are less than those being obtained with crystal mixing methods.

At the present time, there is no absolute power-measuring instrumentation available for measuring power at frequencies above 100 Gc; therefore conversion losses and actual output power of the harmonic generators cannot be measured. Undoubtedly, much research work is

being done to develop power-measuring instrumentation, but very little material has been published about such instrumentation for this area of development.

A source of energy in the millimeter region that is quite easily used is the mercury arc lamp. The mercury arc supplies a wide band of energy from the millimeter region to the ultraviolet, and is a much more convenient source of energy than the metallurgical furnace. In addition, it has been stated that at certain discrete frequencies the output of the mercury arc lamp is known to be an order of magnitude greater than that of a metallurgical furnace.[1] Although no curves have been reported for the output of the mercury lamp as a function of frequency, it is felt that the mercury arc is a useful source of noncoherent energy for submillimeter research.

Since the amount of energy radiated from a blackbody source can be determined from the Planck's law, Eq. 2, blackbody radiation is used for calibration of microwave radiometers. The source commonly used for such radiation is the metallurgical furnace, because elevated temperatures can easily be obtained. The amount of energy that the metallurgical furnace can emit is limited, however, by its maximum temperature of 2000°K. Such a blackbody source has a low output by comparison with most millimeter energy sources; however, it is very good as a calibration tool for other millimeter sources using comparison techniques.

In superheterodyne receivers, a definite local oscillator power is required for optimum mixer operation. A klystron with the necessary power requirements at the higher frequencies is very expensive and not always available, but a method of circumventing part of the problem is to employ a harmonic mixer. Mixer action is obtained by supplying local oscillator power from a klystron that functions at a lower frequency and operates the mixer at a harmonic mode. However, harmonic mixing contributes more noise to the system than does conventional mixing, because more crystal current is required to meet the need for greater local oscillator power.

The efficiencies of harmonic mixers cannot be determined exactly because of the previously mentioned lack of absolute power-measuring equipment at the millimeter frequency. Approximate values for the harmonic generators and harmonic mixers can be determined, however, by calibrating the system at some lower frequency and assuming that the characteristics of the crystal remain the same at the higher frequencies.

---

[1] Private communication to the authors from C. F. Cook, of the NOLC Components and Circuits Branch.

Although the harmonic mixer is steadily increasing the detection capability at higher frequencies, it is an expensive method because many klystrons are required in order to cover the wide spectrum of the millimeter band. At the very short wavelengths, the harmonic mixer becomes impractical also because of waveguide limitations and construction problems. Besides being a narrow-band system, the superheterodyne detector is less sensitive than forms of detection in which the frequency is not converted to a lower frequency. Several of these direct-detection techniques are described in the following paragraphs.

The Golay cell is a thermal detector in which the incident radiation heats a confined volume of gas and expansion of the heated gas displaces a flexible membrane that supports a small mirror. Motion of the membrane is noted by recording the change in a reflected light beam from the moving mirror. Because the flexible membrane is necessarily very delicate, it is subject to two forms of noise. One form is mechanical vibration, which can be reduced, if not eliminated, by mechanical isolation from all vibration. The other source of noise, which determines the minimum detectable energy level, is the Brownian motion of the gas in the cell itself. This limit is equal to or better than that of other thermal detectors, and the cell achieves a time constant of less than 10^{-3} sec. The minimum detectable signal for the Golay cell is approximately 2×10^{-10} watt.

Recently, metal-depositing techniques have been used to form dissimilar conductors and junctions, in an attempt to improve the sensitivity of the thermocouple detector. In this type of detector, thermocouples are connected in series to form a thermopile. The thermocouple junctions are electrically isolated, but are thermally connected to a common target material, upon which the incident radiation impinges. The reference junctions are similarly connected to a common reference-temperature material. The deposition of junction material should decrease the mass sufficiently to give a time constant of less than 0.1 sec. The minimum sensitivity of the thermopile is limited by the Johnson noise of the detector. With reasonable dimensions and a band pass of 1 cps, the minimum sensitivity should be approximately 10^{-11} watt; recent laboratory models have achieved 10^{-10} watt.

Bolometer detectors are based on the change in resistance of a sensitive conductor with a change in temperature. Changes in the bolometer bias current cause changes in potential across the bolometer, which are then detected. The noise contribution from the bolometer is caused by Johnson noise and any instability in bias current. As with all thermal detectors, in the effort to gain maximum efficiency difficulties are usually encountered in matching the incident energy to the sensor; that is, if material is applied to the sensor to absorb all the incident energy, the increased mass causes a decrease in sensitivity for a given time constant.

Recently, a detector has been developed in which the bolometer element is part of a lossy coaxial line (Ref. 14). The energy is coupled to the element by means of a horn and waveguide assembly. Sensitivities of 3×10^{-11} watt have been achieved at 1-mm wavelengths. This method of matching, however, causes the detector to be frequency-dependent, and several detectors are therefore required to cover the millimeter region.

Photoconductive detectors, in which the resistance decreases when electromagnetic radiation impinges upon its semiconductor material, are being thoroughly investigated. Detectors of this type do not rely upon the thermal mass to determine the time constant of the detector as do the previously mentioned thermal detectors. The Putley detector, a photoconductive device covering the millimeter region from approximately 0.2 to 8.6 mm, has recently been described as having a sensitivity of 2×10^{-12} watt with a time constant of less than 1 μsec (Ref. 14). For maximum sensitivity, this detector must be cooled to a temperature of 4.2°K or below and must have a magnetic field on the order of 80,000 gauss. Although it has a sensitivity that compares well with the best thermal detectors, it has a much shorter time constant. This detector is quite expensive, and the requirements of cooling and a magnetic field diminish its attractiveness for portable or mobile applications.

A comparison of the spectral response of these detectors is shown in Fig. 4.

DISCUSSION

There are many areas in which research and experimental work must be done. The operation of submillimeter wave equipment—whether for communication, detection, or research—will require a thorough investigation of the submillimeter characteristics of matter. An area where experimentation is needed is submillimeter energy sources; other laboratories are aware of this need and are working to alleviate the situation. Another area is power-measuring equipment for submillimeter energy; here, because absolute power-measuring equipment is not required for component evaluation, and hence for system design decisions, no immediate solution is foreseen. Optimum detection techniques have not been achieved; further research should be directed toward this goal.

Two other important areas in which experimental work must be done are atmospheric measurements and the characteristics of materials. Atmospheric measurements can be divided into two groups, attenuation and radiation. These measurements are required in order to determine

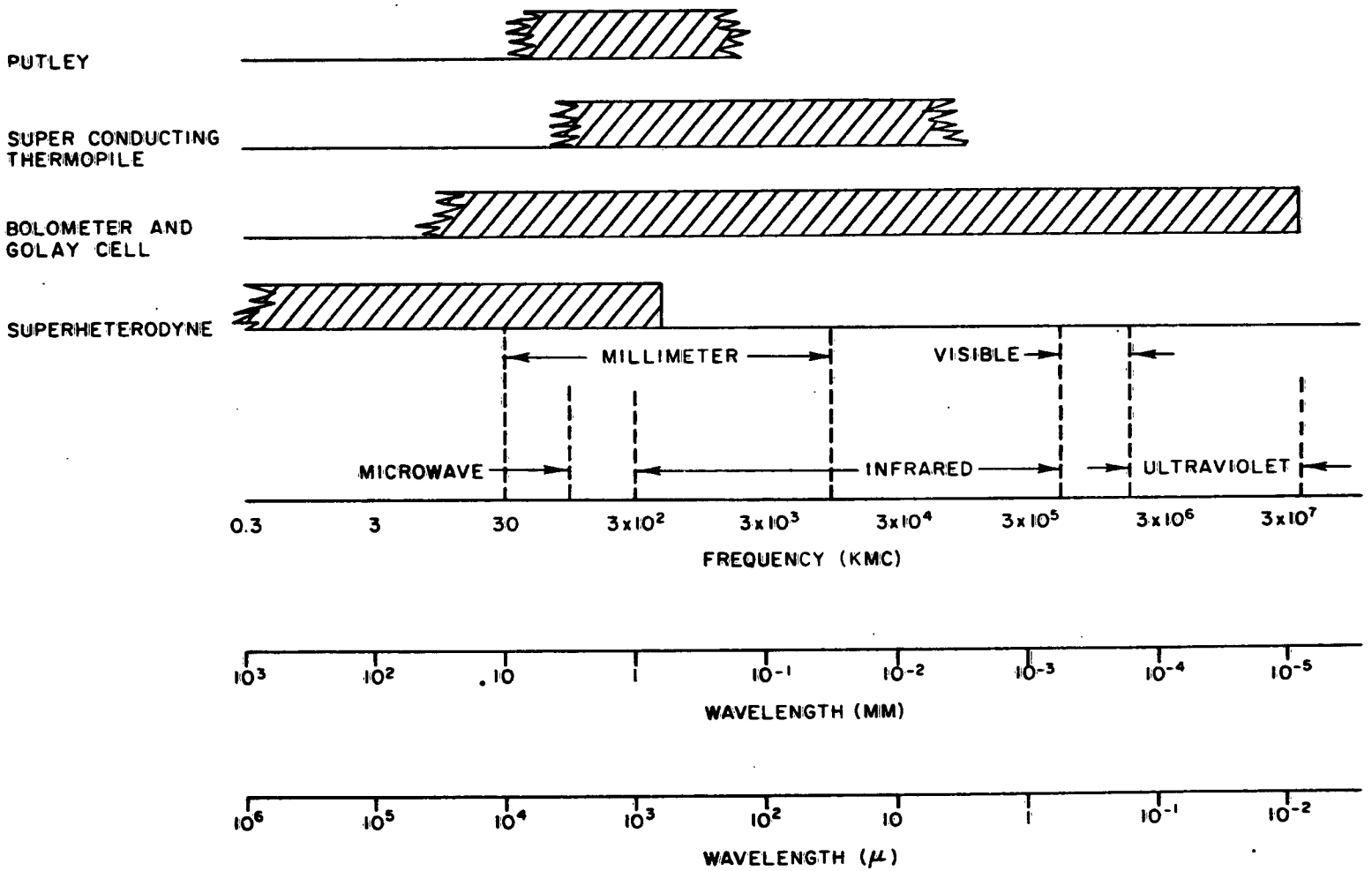

FIGURE 4. Spectral Response of Various Detectors as a Function of Frequency and Wavelength

the effects that must be taken into consideration in the design of equipment that will operate in the atmosphere. Since thermal signals from the atmosphere cannot be measured in the laboratory, a large number of them must be measured under various actual weather conditions to reduce the errors in evaluating the data.

Experimental work on the characteristics of materials may also be divided into two groups. One group pertains to system design and the other to radiation sources involved in radiometer mapping. The materials investigated in the first group should be measured for attenuation, absorption, and dielectric constants as a function of frequency. The results of these measurements could be used to determine what window material, filters, and other dielectric components would be optimum for use in millimeter radiometer, communication, and radar systems. In the second group investigation would be made of the emissivity and reflection coefficients of the different materials that make up the earth's surface. The results of these measurements are necessary in order to evaluate the information obtained from a mapping radiometer.

The first step in setting up a submillimeter research program would be the construction of a submillimeter spectrometer system. The spectrometer should use harmonic generation sources, which would give narrow bandwidths and stable coherent radiation so that the submillimeter wave interaction with matter could be studied in detail. An interferometer in the spectrometer system would give accurate phase measurements, so that the dielectric constants of various materials could be calculated.

The second item to be built for the research program should be an atmospheric absorption test cell. This cell should be about 500 ft long and vacuum-tight, so that atmospheric absorption could be measured as a function of pressure and water-vapor density. The absorption chamber used for the attenuation measurements must be a good submillimeter wave transmission line. The only methods that would work for the chamber are (1) to use a beam waveguide, or (2) to use a large-diameter pipe in which a narrow radiation beam would not encounter much interference from the sides of the pipe. After the required measurements have been made, the effect that the various atmospheric gases have on absorption would be studied. The results of this part of the program would then be used to evaluate the feasibility of using millimeter and submillimeter waves for communication and detection within the earth's atmosphere.

A radiometer could also be used to measure atmospheric radiation. A change in water-vapor density causes a change in atmospheric radiation at a given frequency, and changes in atmospheric radiation allow the radiometer to be used as a tool in the study of atmospheric dynamics.

However, these same variations in radiation have the effect of limiting the use of the radiometer somewhat as a thermal mapping device.

FUTURE PLANS

The Laboratory plans to continue its recently initiated research program for measuring the electrical properties of matter at frequencies greater than 100 Gc. The apparatus used for making these measurements will incorporate both optical and microwave techniques.

The measurement of the reflection, dielectric constant, and the attenuation of this radiation will be started first. The sources and the detectors will use microwave techniques. The methods employed in the measurements will be similar to those used at optical frequencies. A discussion of the particular instrument used will be included in the first report after some of the measurements have been taken. After this part of the measurements program is well under way, it is planned that an atmospheric attenuation measurement program will be started.

The atmospheric attenuation measurements will require a test cell in which atmosphere can be controlled under laboratory conditions and attenuation of the electromagnetic energy propagated through it can be measured. Altitudes will be simulated by partially evacuating the cell. However, for the immediate future, measurements based on these simulated altitudes will be taken at the sea-level temperature at the time of the experiment, since the cost of instrumentation to maintain in the cell the temperatures normally found at the various altitudes is, at this time, prohibitive.

Although initially the measurements will be made at simulated altitudes, fixed temperature, and dry air at the fundamental frequencies of a reflex klystron at millimeter wavelengths, the test cell will be capable of expansion to the submillimeter region by the addition of suitable harmonic generators and various components necessary for optimum operation in that region. In addition, suitable methods will be developed to allow water vapor to be added to the cell so that the increase in attenuation from moisture can be determined under controlled conditions.

The data gathered in these programs will be used to help evaluate the effectiveness of a submillimeter radiometer for use in the earth's atmosphere. Future plans also call for a more comprehensive study program on submillimeter radiometry in the earth's atmosphere.

NOMENCLATURE

A	Effective area of the portion of the antenna covering the target
$A_e(\theta,\phi)$	Effective antenna area
A_t	Area of the target (mks)
B	Beam width of the antenna
b	Symbol used in place of G for the background
c	Speed of light (mks)
$d\Omega$	Differential solid angle
h	Planck's constant (mks)
k	Boltzmann constant (mks)
$P(\lambda,T)\Delta\lambda$	Energy radiated by a blackbody per unit area in 1 sec in 1 steradian
$P_G(\lambda,T_G)\Delta\lambda$	Energy radiated by the gray body G per unit area in 1 sec in 1 steradian
$P_s(\lambda,T_s)\Delta\lambda$	Radiometric measurement of the radiation from the sky
r	Distance between target and radiometer
T	Temperature at which a blackbody would emit $P(\lambda,T)\Delta\lambda$
T_b	Thermodynamic temperature of the background
T_s	Temperature at which a blackbody would emit $P_s(\lambda,T_s)\Delta\lambda$ —called the radiometric temperature of the sky
T_t	Thermodynamic temperature of the target
t	Symbol used in place of G for the target
γ	Atmospheric attenuation
ΔT_{min}	Minimum detectable blackbody temperature change
$\Delta T_{t(min)}$	Minimum detectable target temperature change

$\Delta\lambda$	Change in wavelength
$\Delta\mathbb{P}_{min}$	Minimum detectable power by the radiometer
$\epsilon_G(\lambda)$	Spectral emissivity for gray body G
θ	Look angle of the radiometer
λ	Wavelength in meters
$\rho_G(\lambda)$	Reflection coefficient for gray body G
Ω	Solid angle of the antenna beam
$\mathbb{P}$	Total power received by the antenna
$\mathbb{P}_s$	Power radiated directly into the antenna by the atmosphere

REFERENCES

1. P. W. Kruse, L. D. McGlauchlin, and R. B. McQuistan. Elements of Infrared Technology. New York: Wiley, 1962.

2. Ohio State University Research Foundation. An Analysis of the Interferometric Submillimeter Radiometer, by R. A. Williams and W. S. C. Chang. Columbus, Ohio, 23 July 1962.

3. U. S. Naval Ordnance Laboratory Corona. Some Calculations of Target Temperatures in Microwave Radiometry, by J. O. Hooper and J. W. Battles. (NAVWEPS Report 8140.) Corona, California, 15 March 1963.

4. Radio Corporation of America. The Radio Spectrum From 10 Gc to 300 Gc in Aerospace Communications, by A. Evans, M. P. Bachynski, and A. G. Wacker. (RCA Victor Research Report No. 6-400-4, Contract No. AF 33(616)-7868.) (ASD-TR-61-589; DDC AD-294452.) Montreal, Canada, August 1962.

5. The Microwave Engineers Handbook and Buyers Guide. Brookline, Massachusetts: Horizon House, Inc., 1963.

6. H. Happ, W. Eckhardt, L. Genzel, G. Sperling, and R. Weber. "Crystal Rectifiers as Receivers for Thermal Radiation in the Region 100-1000 μ Wavelength." Z. Naturforsch., Vol. 12-A, June 1957. Pp. 522-24.

7. N. G. Iaroshovskii and A. E. Stanevich. "Rotational Spectrum of Water Vapor and the Absorption of Humid Air in the 40-2500 μ Wavelength Region." Optics and Spectroscopy, Vol. 6, June 1959. Pp. 521-22.

8. H. A. Gebbie. "Detection of Submillimeter Solar Radiation." Phys. Rev., Vol. 107, August 1957. Pp. 1194-95.

9. L. J. Anderson et al. "Attenuation of 1.25 Centimeter Radiation Through Rain." Proc. IRE, Vol. 35, April 1947. P. 351.

10. A. Sommerfeld. Electrodynamics. New York: Academic Press, Inc., 1952. Pp. 177-92.

11. G. Goubau. "Surface Waves and Their Application to Transmission Lines." J. Appl. Phys., Vol. 21, November 1950. Pp. 1119-28.

12. G. Goubau and F. Schwering. "On the Guided Propagation of Electromagnetic Wave Beams." Trans. IRE, Vol. AP-9, May 1961. Pp. 248-56.

13. J. R. Christian and G. Goubau. "Experimental Studies on a Beam Waveguide for Millimeter Waves." Trans. IRE, Vol. AP-9, May 1961. Pp. 256-63.

14. J. F. Byrne and C. F. Cook. "Microwave Type Bolometer for Submillimeter Wave Measurements," paper presented at IRE Millimeter and Submillimeter Conference, Orlando, Florida, January 1963.

15. E. H. Putley. "Impurity Photoconductivity in N-Type In-Sb." J. Phys. Chem. Solids, Vol. 22, 1961. Pp. 241-47.

Naval Ordnance Laboratory Corona. (NAVWEPS Report 8169)
SUBMILLIMETER RADIOMETRY, by J. W. Battles and D. E. Crane, Research Department. 1 November 1963. 32 pp. UNCLASSIFIED

This report discusses some of the problems involved in defining the parameters of a submillimeter radiometer. Areas in which there is a need for experimental measurements are outlined, a short survey is given of millimeter and submillimeter wave components, and future plans of the submillimeter research program are discussed.

1. Radiometers—Applications
I. Title
II. Battles, J. W.
III. Crane, D. E.

WepTask: R360-FR-104/211-1/R011-01-001

This card is UNCLASSIFIED

Naval Ordnance Laboratory Corona. (NAVWEPS Report 8169)
SUBMILLIMETER RADIOMETRY, by J. W. Battles and D. E. Crane, Research Department. 1 November 1963. 32 pp. UNCLASSIFIED

This report discusses some of the problems involved in defining the parameters of a submillimeter radiometer. Areas in which there is a need for experimental measurements are outlined, a short survey is given of millimeter and submillimeter wave components, and future plans of the submillimeter research program are discussed.

1. Radiometers—Applications
I. Title
II. Battles, J. W.
III. Crane, D. E.

WepTask: R360-FR-104/211-1/R011-01-001

This card is UNCLASSIFIED

Naval Ordnance Laboratory Corona. (NAVWEPS Report 8169)
SUBMILLIMETER RADIOMETRY, by J. W. Battles and D. E. Crane, Research Department. 1 November 1963. 32 pp. UNCLASSIFIED

This report discusses some of the problems involved in defining the parameters of a submillimeter radiometer. Areas in which there is a need for experimental measurements are outlined, a short survey is given of millimeter and submillimeter wave components, and future plans of the submillimeter research program are discussed.

1. Radiometer—Applications
I. Title
II. Battles, J. W.
III. Crane, D. E.

WepTask: R360-FR-104/211-1/R011-01-001

This card is UNCLASSIFIED

Naval Ordnance Laboratory Corona. (NAVWEPS Report 8169)
SUBMILLIMETER RADIOMETRY, by J. W. Battles and D. E. Crane, Research Department. 1 November 1963. 32 pp. UNCLASSIFIED

This report discusses some of the problems involved in defining the parameters of a submillimeter radiometer. Areas in which there is a need for experimental measurements are outlined, a short survey is given of millimeter and submillimeter wave components, and future plans of the submillimeter research program are discussed.

1. Radiometers—Applications
I. Title
II. Battles, J. W.
III. Crane, D. E.

WepTask: R360-FR-104/211-1/R011-01-001

This card is UNCLASSIFIED

NAVWEPS Report 8169; WepTask R360-FR-104/211-1/R011-01-001.

INITIAL DISTRIBUTION

	Copies
Chief, Bureau of Naval Weapons Navy Department Washington 25, D. C. 20360	
Attn: Code R-12, Dr. Lamar	1
RM-12, Dr. Tanczos	1
RMGA-41, J. Lee	1
RMWC-421, C. Francis	1
RMWC-422, D. Armstrong	1
SP-001	1
DLI-31	4
U. S. Naval Weapons Services Office U. S. Naval Base Philadelphia, Pa. 19112	2
Defense Documentation Center Building No. 5 Cameron Station Alexandria, Va.	20
NOLC:	
C. J. Humphreys, Code RR	1
F. C. Essig, Code RRE	1
J. W. Battles, Code RREM	1
D. E. Crane, Code RREM	1
H. A. Johnson, Code RREM	1
R. P. Moore, Code RREM	1
F. C. Alpers, Code RM-2	1
W. F. Meggers, Jr., Code RMG	1
Technical Library, Code ADIL	2